ACS OMEGA

Open Access

http://pubs.acs.org/journal/acsodf

Article

pH-Sensitive Hydrogels Fabricated with Hyaluronic Acid as a Polymer for Site-Specific Delivery of Mesalamine

Huma Liaqat, Syed Faisal Badshah,* Muhammad Usman Minhas, Kashif Barkat, Saeed Ahmad Khan, Muhammad Delwar Hussain, and Mohsin Kazi

Cite This: *ACS Omega* 2024, 9, 28827−28840

Read Online

ACCESS | Metrics & More | Article Recommendations

ABSTRACT: Hydrogels with the main objective of releasing mesalamine (5-aminosalicylic acid) in the colon in a modified manner were formulated in the present work using a free-radical polymerization approach. Different ratios of hyaluronic acid were cross-linked with methacrylic and acrylic acids using methylenebis(acrylamide). The development of a new polymeric network and the successful loading of drug were revealed by Fourier transform infrared spectroscopy. Thermogravimetric analysis demonstrated that the hydrogel was more thermally stable than the pure polymer and drug. Scanning electron microscopy (SEM) revealed a rough and hard surface which was relatively suitable for efficient loading of drug and significant penetration of dissolution medium inside the polymeric system. Studies on swelling and drug release were conducted at 37 °C in acidic and basic conditions (pH 1.2, 4.5, 6.8, and 7.4, respectively). Significant swelling and drug release occurred at pH 7.4. Swelling, drug loading, drug release, and gel fraction of the hydrogels increased with increasing hyaluronic acid, methacrylic acid, and acrylic acid concentrations, while the sol fraction decreased. Results obtained from the toxicity study proved the formulated system to be safe for biological systems. The pH-sensitive hydrogels have the potential to be beneficial for colon targeting due to their pH sensitivity and biodegradability. Inflammatory bowel disease may respond better to hydrogel treatment as compared to conventional dosage forms. Specific amount of drug is released from hydrogels at specific intervals to maintain its therapeutic concentration at the required level.

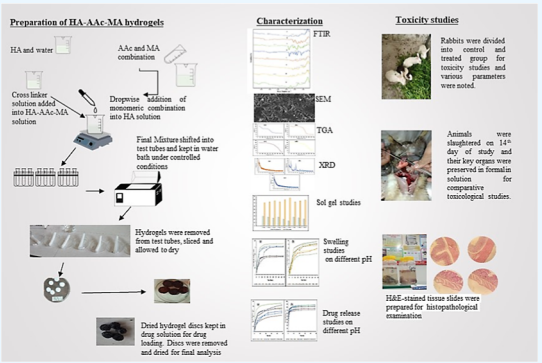

1. INTRODUCTION

Crohn's disease (CD) and ulcerative colitis (UC) are examples of inflammatory bowel diseases (IBDs). The majority of patients with these conditions require long-term drug therapy to achieve and maintain remission. The aforementioned therapies reduce the likelihood of recurrence and minimize the need for corticosteroids, long-term inpatient therapy, and surgical procedures.[1] For approximately 30 years, patients with UC have relied on mesalamine also known as 5-aminosalicylic acid (5-ASA) as their primary treatment.[2] Traditional therapies for CD and UC include 5-ASA, corticosteroids, sulfasalazine, thiopurines, and methotrexate. 5-ASA, an anti-inflammatory medicine, is the oldest and preferred treatment for various kinds of IBD. It may also be a safe and effective treatment for mild to moderate UC. It has also been reported that substantial dosages of oral, rectal, or mixed dosage formulations of 5-ASA can be used to treat active UC. This drug also protects against colorectal cancer.[3] The standard dose of 5-ASA is typically fast, and 5-ASA is significantly absorbed in the upper digestive tract when taken orally. This absorption may result in the onset of numerous undesirable effects, as well as a low local drug concentration in the intestinal region and, as a result, a poor therapeutic effectiveness for IBD. Focusing on 5-ASA release to the colon will thereby alleviate these issues.[4]

Controlled release drug delivery systems differ from typical formulations in that nearly all of the loaded drug(s) are released abruptly and uncontrollably. Preparation with an integrated technology to govern drug release kinetics over time is referred to as "controlled release drug delivery system" or a "controlled drug delivery system".[5] Controlled drug release systems (CDRSs) have received much attention in recent decades since they have transformed several current drugs into more potent treatments. CDRSs are designed to modify drug release kinetics to maximize therapeutic advantages while decreasing undesirable effects.[6] Obtaining the specific concentration of therapeutic agent is hard to achieve and hence results in failure of the therapy.[7] Conventional systems typically

Received: April 4, 2024
Revised: June 1, 2024
Accepted: June 6, 2024
Published: June 21, 2024

acquire high plasma drug concentrations after administration and rapidly release their payload, which then decreases due to the elimination process. Finally, this causes variable drug concentrations in the plasma and the demand for frequent administration, which renders the patient at risk of toxicity and has less efficient therapeutic implications. The fundamental objectives of the controlled release and targeted administration of drugs are to overcome the short half-life, nonspecific dispersion, and off-target toxicity of conventional drugs. Patients with chronic illnesses such as cancer, arthritis, and ulcers that require treatment for weeks, months, or even years benefit substantially from CDRSs. Several dosage forms and carrier systems have been examined for their controlled release qualities as CDRS research has progressed. Because of advances in disease understanding and imaging tools, scientists are able to develop drug delivery systems that target a particular disease site or tissue. These targeted techniques take advantage of specific conditions and tissue characteristics, such as leaky vasculature or receptor overexpression, or the drug delivery mechanism itself, such as particle size, and encourage preferential accumulation. The two most captivating applications of nanoparticle-based systems that have recently been researched are controlled release and targeted delivery of the therapeutic payload. Managing drug release kinetics has advantages such as extended therapeutic effects, decreased dosing frequency, fewer fluctuations in plasma levels, and fewer side effects, whereas targeted delivery has advantages such as enhanced drug accumulation at the site of action and reduced off-target toxicity, which improves chronic disease management.[8] Hydrogels are a class of biomaterial consisting of a three-dimensional polymeric network with a significant proportion of aqueous phase. The network is prevented from dissolving by physical and chemical interactions resulting from the presence of cross-links.[9] In response to the increasing interest in personalized medicine and precision medicines, smart biomaterials have recently been developed.[10] The formulation of gels can be triggered by a variety of stimuli, such as ionic strength, temperature, and pH.[11] Stimulus-responsive hydrogels can be considered smart biomaterials that can release pharmaceuticals in reaction to external stimuli such as pH, temperature, electrical and magnetic fields, light, and biomolecule concentration.[12] The macroscopic and physical properties of smart hydrogels change in response to an external trigger.[13] Smart hydrogels can be utilized in drug delivery systems to reduce dosing frequency, maintain therapeutic concentrations in a single dose, and limit side effects by limiting drug buildup in tissues other than the target locations.[14] Smart hydrogels are an excellent choice for drug-containing extended-release systems owing to their ease of preparation.[15] Biopolymers are naturally occurring and are produced during the life cycle of green plants, bacteria, fungi, and animals. As they are safe and natural, they have attracted great attention in the field of drug delivery and medicine.[16] Because biopolymers are biocompatible and nontoxic, they are a better alternative for generating self-healing polycomplexes than synthetic polymers. Hyaluronic acid (HA), a high-molecular-weight linear glycosaminoglycan, is composed of repeating disaccharide molecules of β-(1,4)-D-glucuronic acid and β-(1,3)-*N*-acetyl-D-glucosamine. It is a weak polyanion with a pK_a of 2.9, biocompatible, viscoelastic, and nontoxic; it also has a high hydrophilicity, lubricant, and moisturizing nature, which aids in increasing biocompatibility and limiting biofilm formation.[17] Tissue engineering, viscosupplementation, and drug delivery are just a few of the many uses for HA. The body releases hyaluronic acid in the initial phases of inflammation as a safeguarding response against the damaging effects of bacterial hyaluronidase and the development of edema. During the process of embryonic development, wound healing, and tumor development, the body's level of hyaluronic acid increases swiftly. HA has a wide range of protective properties, making it a valuable anti-inflammatory and antiedematous agent. Its ability to inhibit the proliferation of epithelial cells is contingent upon both its molecular weight and concentration. Scavenging prostaglandin, metalloproteinase, and other bioactive molecules, hyaluronic acid, might function as an anti-inflammatory agent, thus lower the concentration of inflammatory mediators, and this anti-inflammatory activity may also play a major role in preventing gastric ulcers. Multiple studies indicate HA's beneficial antioxidant properties. Reactive oxygen intermediates (ROIs) can cause injuries to tissues; however, HA can lessen this damage by forming mechanical barrier that prevents ROIs from reaching the cell surface, minimizing DNA damage, NF-kB activation, and caspase activation.[18]

Previous reports have discussed the use of HA as a mucoadhesive biopolymer. Zeta potential plays crucial role in the comprehension and explanation of particle interactions. The mucoadhesive, mucopenetration, and cell uptake properties in mucosal delivery of drugs are influenced by the surface charge. It has been demonstrated that the negatively charged particles improve cellular absorption by interactions with positively charged lipid membrane groups and improve mucopenetration by limiting interactions with the negatively charged components of mucus. The zeta potentials of HA had comparatively elevated negative charge values, suggesting that it has the ability to augment drug penetration.[19] In terms of usage, oral administration is the most preferred approach in daily life. However, following oral administration of conventional pharmaceutical preparations, the majority of the drugs are released and absorbed in the stomach and small intestine, with relatively little amount reaching the colon. As a result, the lesion site frequently fails to achieve the effective drug concentration required for treatment. Researchers have focused a lot of interest in colon-specific drug delivery systems (also known as CDDSs) since they can target and release medications in the colon and have a good therapeutic effect on colon disorders. The most commonly used CDDS at the moment is the pH-sensitive oral CDDS, which is primarily made based on variations in the pH of the gastrointestinal system. The pH of the stomach is typically around 1.2, duodenum is roughly 4.5, end of the small intestine's is 6−6.8, and that of the colon is 6.5−7.5. Hydrogels are thought to be the perfect oral drug delivery method due to its many unmatched benefits, which include improved stability, easy preparation, and high drug-loading efficiency. Colon-specific drug release can be accomplished using hydrogels with various designs. In a nut shell, the carrier material does not dissolve and slightly swells in the upper gastrointestinal system (a low pH environment), which results in less drug release, but the carrier material gradually dissolves and promotes drug release in the colon (a high pH environment).[20] Numerous studies have focused on the development of delivery systems that specifically target the colon to improve the treatment of IBD. The best 5-ASA colonic administration strategy should optimize drug distribution to the colon while minimizing its systemic absorption in the upper tract of the gut. There are

https://doi.org/10.1021/acsomega.4c03240
ACS Omega 2024, 9, 28827−28840

currently few rectal and oral formulations available that aid in delivering 5-ASA to the colon. Considering 5-ASA as a hydrophobic drug, the hydrogel-based 5-ASA delivery approach can address the challenges of low solubility and poor adhesion. Hydrogel delivery can improve the effectiveness of 5-ASA and treat UC by overcoming the limited solubility and poor adhesion associated with the current 5-ASA delivery systems.[21] The solubility of 5-ASA also known as mesalamine in the polymeric system was enhanced by the utilization of natural polymers, which was anticipated to be linked with increased wetting, adsorption, and decreased crystallinity.[22]

The goal of this research was to create a new polymeric hydrogel system for oral administration with promising properties that imparted a controlled release effect of 5-ASA in vitro and to optimize a novel drug delivery system for pharmaceutical applications with reduced dosage frequency, patient compliance, and safety.

2. EXPERIMENTAL SECTION

2.1. Materials. 5-amino salicylic acid (mesalamine), hyaluronic acid, acrylic acid, methacrylic acid, *N*,*N*-methyl-enebisacrylamide, ammonium persulfate, ethanol, hydrochloric acid, potassium dihydrogen phosphate, sodium hydroxide, and potassium chloride were purchased from Sigma-Aldrich Chemie GmbH (Steinheim, Germany). All the compounds were of analytical grade.

2.2. Methods. *2.2.1. Fabrication of Hydrogels.* Hydrogels were synthesized by employing the free-radical polymerization method with slight modification in previously published guidelines.[23] A precise amount of the polymer hyaluronic acid was added to a beaker along with the precise amount of water (solvent), and the mixture was constantly swirled for 30 min using magnetic stirring. Methacrylic acid and acrylic acid were quantified and blended in a beaker before being introduced to the polymer solution drop by drop and allowed to stir for 10 cycles. Water was added to a certain amount of ammonium per sulfate (APS) in a separate beaker to form a solution. Then, the APS solution was added to the polymer/monomer solution and agitated for 10 min. In a separate beaker, water was added to a measured amount of methylene bis acrylamide (MBA), and the mixture was constantly stirred until a clear solution was obtained. The combination of polymers, monomers, and initiators was then mixed with the MBA solution for 5 min. The final mixture was placed in marked glass test tubes, wrapped in aluminum foil, and placed in a preheated water bath set at 55 °C for the first hour and 60 °C for the next 2 h. A total number of nine formulations were prepared with varying concentrations of polymers, monomers, and cross-linkers, as shown in Table 1.

2.2.2. Washing and Cutting. After being removed from the water bath, the test tubes containing the hydrogels were allowed to cool to room temperature. After removal from the test tubes, the solid cylindrical hydrogels were rinsed with a 50:50 solution of water and ethanol to remove any remaining impurities and finally precisely sliced into small, 9 mm thick discs. The discs were placed in Petri dishes in vacuum oven at 40 °C for a week to get dried hydrogel discs.

2.2.3. Characterizations. 2.2.3.1. Scanning Electron Microscopy (SEM). The most extensively documented technique for describing hydrogel microarchitectures is scanning electron microscopy (SEM). This high-resolution imaging tool offers a precise, nanoscale image of the hydrogel surface. SEM is an electron-based technique in which a metal-coated specimen is bombarded with primary electrons from a high intensity beam, referred to as "electron gun", which causes secondary and backscattered electrons to be emitted. While backscattered electrons create contrast between regions with different chemical compositions, secondary electrons highlight attention to the specimen's form and topography. High vacuum is required for SEM imaging because gas can weaken electron beams and prevent them from scattering. Hydrogel pore size, pore distribution, porosity percentage, fiber thickness, and fiber orientation are all measured using SEM microphotographs.[24]

Using SEM (JEOL Japan Mode: J8M 6480LV), the surface morphology of the hydrogels loaded with 5-ASA was examined. Following their splitting, the dried hydrogel discs were positioned on the double-stick tape fastened to an aluminum stub. The stubs were coated with gold using a gold sputter module in a high-vacuum evaporator while the region was filled with argon before imaging. SEM was the most effective tool for analyzing the surface configurations. The surface morphology of the materials was visualized by recording micrographs and scanning them at different resolutions.[25]

2.2.3.2. Thermal Analysis. A TGA-modules Q5000 series thermal analysis system was utilized to evaluate the thermal stability of the hydrogels and the pure reactants. After being crushed, the hydrogel samples were passed through a 40-grit screen. Weight fluctuations were evaluated in relation to the higher temperature after the samples (5−10 mg) were processed at a temperature range of 500 °C with heating at a rate of 20 °C/min in a dynamic nitrogen atmosphere.[25]

2.2.3.3. Fourier Transform Infrared (FTIR) Spectroscopy. FTIR was used to evaluate a range of drug−polymer interactions, compatibility, and polymeric network formation of the raw materials to target the cross-linking required to complete hydrogel synthesis.[26] The hydrogel discs were thoroughly crushed before being passed through sieve no. 40.[27] Monomers (methacrylic acid and acrylic acid), unloaded and loaded hydrogel discs, and polymer (hyaluronic acid) were placed on a zinc selenide crystal, and the assembly was rotated and scanned with attenuated total reflectance-Fourier transform infrared spectroscopy (ATR-FTIR). The FTIR spectra of the compounds were recorded in the 4000−650 cm^{-1} range.

2.2.3.4. Powder X-ray Diffraction Studies. Powder X-ray diffraction (PXRD) is a nondestructive technique that uses the diffraction patterns to show the atomic arrangements of a structure in order to define and characterize different

Table 1. Concentrations of Ingredients in Combination Monomer-Based Hydrogel Formulations

formulation code	the concentration of polymers, monomers, cross-linkers, and initiator				
	hyaluronic acid (g)	acrylic acid (g)	methacrylic acid (g)	MBA (g)	APS (g)
CM-1	0.04	2	2	0.05	0.2
CM-2	0.05	2	2	0.05	0.2
CM-3	0.06	2	2	0.05	0.2
CM-4	0.05	2	2	0.05	0.2
CM-5	0.05	2.5	2.5	0.05	0.2
CM-6	0.05	3	3	0.05	0.2
CM-7	0.05	2	2	0.05	0.2
CM-8	0.05	2	2	0.06	0.2
CM-9	0.05	2	2	0.07	0.2

https://doi.org/10.1021/acsomega.4c03240
ACS Omega 2024, 9, 28827−28840

crystalline materials.[28] PXRD was used to examine the crystalline and amorphous characteristics of the drug, polymer, and drug-loaded hydrogels. Sharp peaks in a compound indicate its crystallinity, whereas diffuse peaks signify the compound's amorphous nature. Glass slides were used to level the weighed crushed samples after they had been put in a sample container.[29] The samples were scanned across the range of 5−50° 2θ at a rate of 1° 2θ/min using a copper Kα radiation source with 1 mm slits and a wavelength of 1.542 Å.

2.2.3.5. Sol−Gel Fraction. The percentage of non-cross-linked segments was determined by means of a sol−gel study. Using 100 mL of distilled water as a solvent, weighed hydrogel discs were extracted using the Soxhlet method for 4 h at 80 °C. To achieve a consistent weight, the extracted gels were dried once more in a vacuum oven set to 40 °C for the required period of time to obtain a constant weight.[30]

Following equations were used to determine the sol and gel fractions. The initial weight of the hydrogel before Soxhlet extraction is denoted by W_o, while the weight of the dried hydrogel after Soxhlet extraction is denoted by W_1.

$$\text{Sol fraction } (\%) = \frac{W_o - W_1}{W_1} \times 100$$

$$\text{Gel fraction } (\%) = 100 - \text{Sol fraction}$$

2.2.3.6. Swelling Studies. To determine how hydrogels respond to pH variations, swelling studies in acidic and basic media were performed. Dried hydrogel discs with known masses were dunk in 50 mL of buffer (pH 1.2, 4.5, 6.8, and 7.4) that was provided in containers with clear labels.[31] At various time intervals, swollen discs were removed from their respective solvents, placed on bloating paper to remove any remaining swelling medium, and weighed using an analytical weighing scale to determine the final weight of the discs.

$$\text{Swelling index } Q = \frac{M_s}{M_d}$$

$$\text{Equilibrium water content } EWC\% = \frac{M_{eq} - M_d}{M_d} \times 100$$

where M_d is the initial weight of the dried hydrogel and M_s is the weight of the swollen hydrogel disc at time t.

2.2.3.7. Polymer Volume Fraction. The amount of polymer that is fully swollen is represented by the polymer volume fraction, or v_2, s. The volume fraction of the polymer at pH 1.2 and 7.4 under completely swelled conditions was calculated using equilibrium volume swelling (V_{eq}). To calculate v_2, the following equation was used

$$v_2,\ s = \frac{1}{V_{eq}}$$

2.2.3.8. Percent Water Content. The hydrophilic nature of hydrogels enables them to absorb solvents with great capacity. The amount of loaded drug within the polymeric network is one of the many variables that may affect the absorbed solvent. The hydrogels' percentage water content was computed in order to determine the exact ratios. This was achieved by taking 500 mg of moist hydrogels in designated Petri dishes with average weight of 40.14 g and placing them in an oven for 24 h at 110 °C ± 5.0. After 24 h, the hydrogel surfaces were checked to be dry by placing the blotting paper. Following the drying process, the Petri dishes were removed from the oven, sealed with a lid, and allowed to cool thoroughly in a desiccator. After the Petri dishes were removed from the desiccator, their lids were removed, and they were weighed for the final time.[32] The following equation was used to determine the water content of the hydrogels

$$w = [(M_{cms} - M_{cds})/(M_{cds} - M_c)] \times 100$$
$$= (M_w/M_s) \times 100$$

where

- w = water content,%,
- M_{cms} = mass of container and moist specimen, g;
- M_{cds} = mass of container and oven-dried specimen, g;
- M_c = mass of container, g,
- M_w = mass of water($M_w = M_{cms} - M_{cds}$), g,
- M_s = mass of oven-dried specimen ($M_s = M_{cds} - M_c$), g

2.2.3.9. Drug Loading. 5-Amino salicylic acid was loaded into the hydrogel discs using the post drug-loading technique through the swelling and diffusion. Phosphate buffer with a pH of 7.4 containing a specified quantity of drug was stirred at room temperature to yield a 1% drug solution. The hydrogel discs were submerged in the drug solution for 5 days. Following removal from the drug solution, the hydrogel discs were blotted with filter paper and rinsed with distilled water to eliminate any remaining drug from their surface. This process occurs when the hydrogel discs have reached equilibrium loading and swelling. The discs were subsequently dried at 40 °C in a vacuum oven until their weight remained constant.[33] The quantity of drug contained in the hydrogels was determined with the given equation.

$$\text{Drug-loaded quantity} = \text{DL} - \text{DUL}$$

The weight of the drug-loaded hydrogel discs is represented by DL, while the weight of the unloaded hydrogel discs is represented by DUL.

2.2.3.10. Percent Drug-Loaded Contents. After being weighed with a dry, clean mortar and pestle, the crushed hydrogel discs were placed in 500 mL of 7.4 pH phosphate buffer solution at 37 °C ± 0.5 °C for 24 h. After that, the mixture was centrifuged at 3000 rpm.[25] The supernatant layer was collected and filtered through 0.45 μm filter paper after centrifugation. An UV spectrophotometer with a maximum wavelength of 218 nm was used to conduct the 5-amino salicylic acid assay. The following formula was used to determine the percentage of drug loading.

$$\text{Percent drug} - \text{loaded content} = \frac{\text{Weight of drug in hydrogel (mg)}}{\text{Weight of dried crusehed hydrogel (mg)}} \times 100$$

2.2.3.11. In Vitro Release Studies. Drug release studies were conducted using a USP dissolution apparatus II (DIS-08S) to determine how drug release is influenced by pH.[34] Release studies were carried out in buffers with pH of 1.2, 4.5, 6.8, and 7.4 in order to examine the pH-dependent release behavior of 5-amino salicylic acid from hydrogels. The weighed hydrogel discs were added to 900 mL of buffer (pH of 1.2, 4.5, 6.8, and 7.4) to mimic gastrointestinal conditions. The paddle speed was set to 50 rpm, and the temperature was 37 °C. To maintain the sink condition, a 5 mL sample was obtained at specific intervals, and the same amount of fresh medium was added. Every sample underwent a triple UV analysis with a

https://doi.org/10.1021/acsomega.4c03240
ACS Omega 2024, 9, 28827−28840

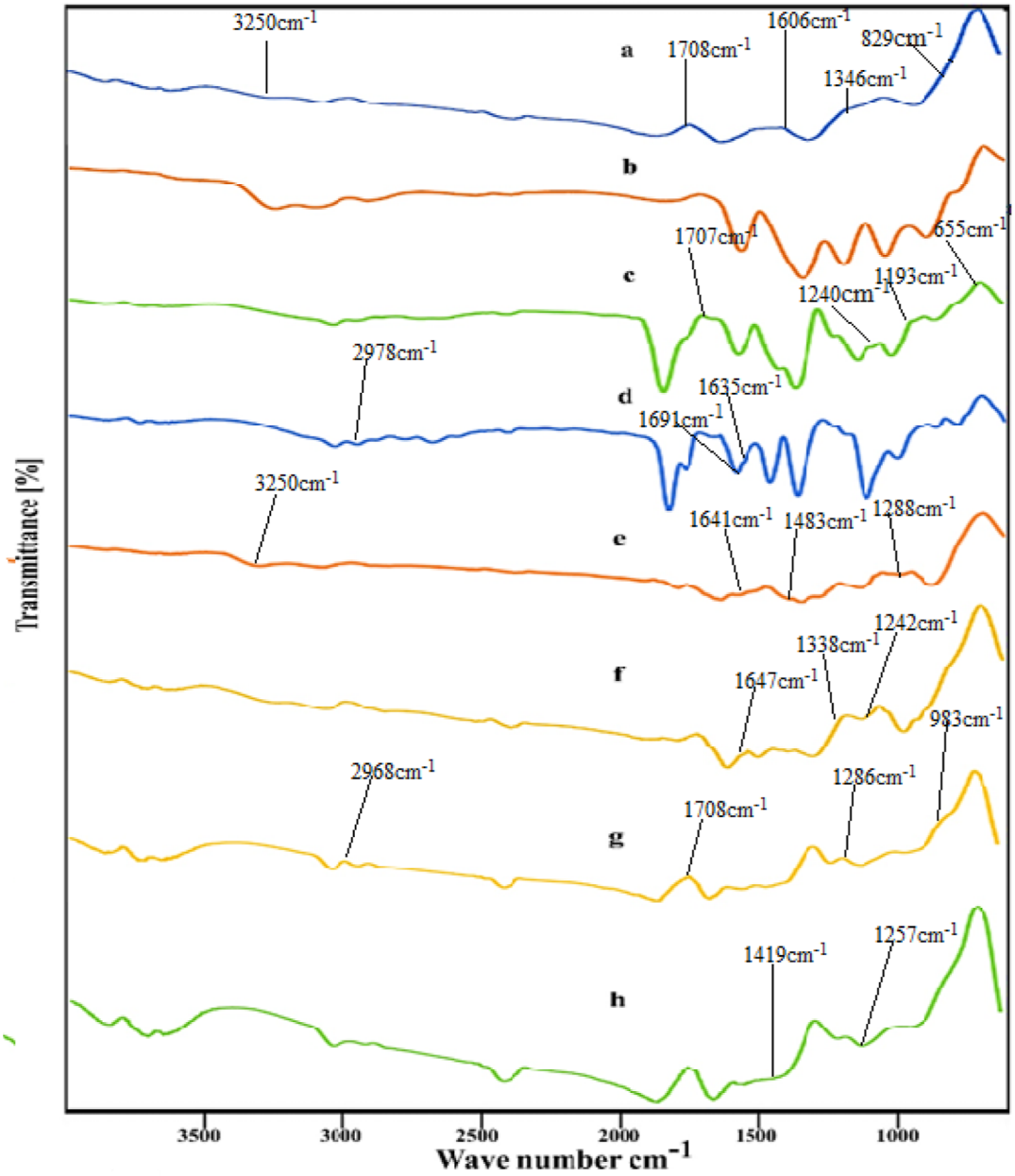

Figure 1. FTIR spectra of the polymer (a), initiator (b), monomers AAC (c) and MA (d), cross-linker (e), drug (f), unloaded hydrogel (g), and drug-loaded hydrogel (h).

maximum wavelength of 218 nm. By correlating in vitro release studies of the hydrogels with release investigations of commercially available 5-amino salicylic acid tablets, we were able to ascertain the effectiveness of developed hydrogels.

2.2.3.12. Biocompatibility Evaluation. A biocompatibility analysis was conducted to assess the toxicity of the hydrogels. For the conduction of this study, the guidelines as approved by the Institutional Research Ethics Committee (IREC) of Faculty of Pharmacy, The University of Lahore, Pakistan for handling and care of animals under the reference number IREC-2023-60 were followed. To conduct this investigation, six (06) healthy rabbits weighing between 1.5 and 2.0 kg were selected and segregated into two groups. The first group was designated the control group, and the second was designated the experimental group. The experimental group received hydrogels at a dose of 2 g/kg in addition to food and water, while the control group received water and food. The distinctive attributes of the two sets of rabbits were noted while they resided in controlled conditions. Blood samples were collected for hematological studies after 14 days of quarantine, and after the rabbits were slaughtered, vital organs from each group were removed and preserved in formalin for the histological examination.[35]

3. RESULTS AND DISCUSSION

3.1. Fourier Transform Infrared (FTIR) Spectroscopy. FTIR spectra of polymer (a), initiator (b), monomers (c,d), cross-linker (e), drug (f), unloaded (g), and drug-loaded hydrogel (h) have been depicted in Figure 1. According to the FTIR spectrum of hyaluronic acid, the strong band at 3250 cm^{-1} was attributed to hydrogen bonding, O−H and N−H vibrations for *N*-acetyl side-chain stretching. Overlapping bands of moderate intensity were evident at 2972 cm^{-1} due

https://doi.org/10.1021/acsomega.4c03240
ACS Omega 2024, 9, 28827−28840

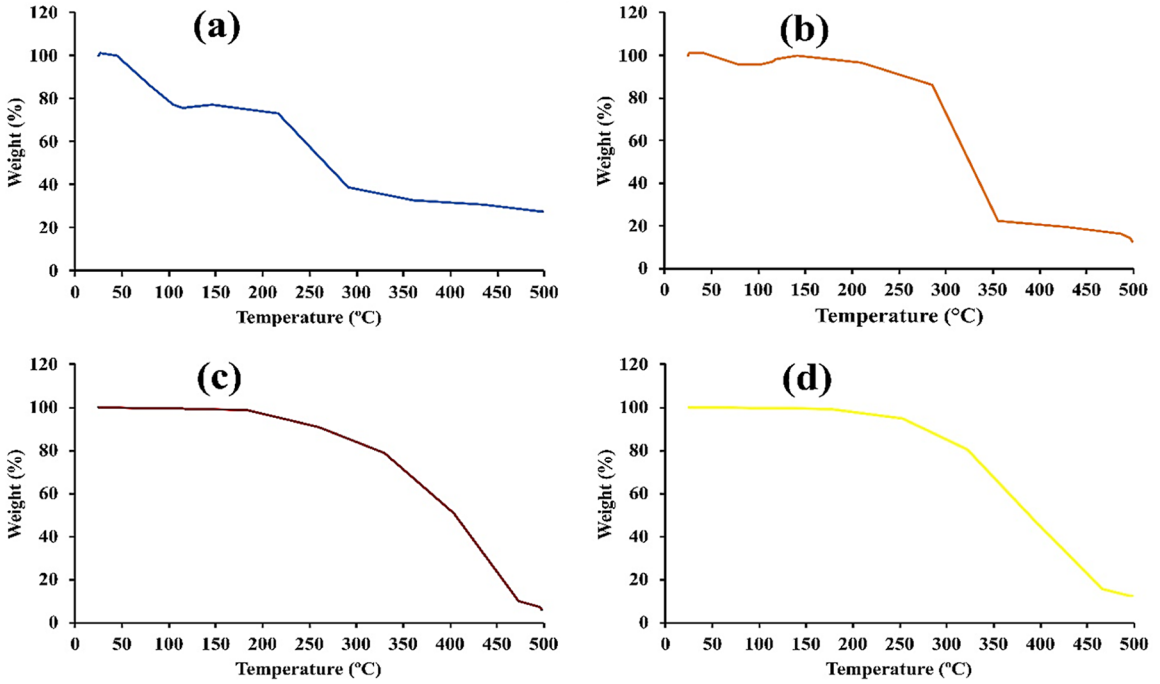

Figure 2. Thermogravimetric analysis of the polymers (a), drugs (b), and unloaded and loaded hydrogels (c, d).

to C−H stretching vibrations. The bands at 1708 and 1452 cm^{-1} were attributed to the asymmetric (C═O) and symmetric (C−O) stretching modes of the planar carboxyl groups in hyaluronate. The amide I and II bands exhibited absorption bands at approximately 1606 and 1346 cm^{-1}, respectively. The 829 cm^{-1} band corresponds to an asymmetrical out-of-phase ring vibration.[36] Peaks in the AAc spectrum were found at 2981 and 1707 cm^{-1}, indicating the presence of $-CH_2$ and −C−C functional groups. Other AAc peaks were found at 1240 and 1193 cm^{-1}, which are attributed to −OH bending and −C−H bending vibrations, respectively, and at 655 cm^{-1}, −C═O stretching was observed.

The peak at 2978 cm^{-1} in the FTIR spectrum of MA indicated the presence of methyl C−H asymmetric stretching. The peaks at 1691 and 1635 cm^{-1} correspond to carboxylic acid stretching vibrations and the presence of a C═C functional group. The FTIR spectra of MBA exhibit N−H groups at 3250 cm^{-1}, C═O groups at 1641 cm^{-1}, and C═C groups at 1483 cm^{-1}.[37] In the FTIR spectrum of MBA, the peak associated with C−N appears at 1288 cm^{-1}.[38] Similarly, the FTIR spectra of 5-amino salicylic acid revealed unique peaks at 1647 and 1571 cm^{-1}, corresponding to COOH and NH_2 stretching and bending, respectively. Similarly, two peaks at 1338 and 1242 cm^{-1} suggested C−N and −OH group stretching and bending, respectively.[33] The chemical interactions of hydrogel constituents such as hyaluronic acid, MBA, AAc, MAA, and APS shifted the positions of their corresponding peaks. Unloaded hydrogel discs of HA-AAc-MA: the bands at 1707 and 1471 cm^{-1} were modified. Similarly, the AAc peaks in the spectra of the hydrogels ranged from 2981, 1707, and 1240 to 2968, 1708, and 1286 cm^{-1}, respectively. Similarly, the peaks of MBA in the spectra of the hydrogels ranged from 1288 and 478 to 1286 and 482 cm^{-1}. The MA peaks shifted from 983 and 929 to 983 and 921 cm^{-1}, respectively.

Cross-linking was attributed to the slightly altered peaks of different components, such as polymers and monomers, which confirmed the efficient polymerization of the generated hydrogels, as proven by FTIR spectrum analysis of an unloaded HA-AAc-MA -based hydrogel. This shifting, abduction, and development of new peaks indicated successful cross-linking of AAc and MA over the backbone of HA; therefore, we may conclude from the FTIR spectrum of the new polymeric network of the hydrogel. Furthermore, the lack of a wavenumber in the FTIR spectra indicating the presence of C═C groups on the product revealed that the graft copolymerization reaction between HA and a combination of methacrylic acid and acrylic acid was successful and occurred in the C═C group.[37] Similarly, with 5-amino salicylic acid, the peaks at 1338 and 1242 cm^{-1} were amplified and shifted to 1419 and 1257 cm^{-1}, indicating better hydrogen bonding and successful drug loading in the hydrogels.[33] These changes in the peak-characteristic bands were observed when 5-amino salicylic acid was integrated into the HA-AAc-MA gels to form the HA-AAc-MA-5ASA polymeric system, indicating its successful loading in the polymeric system.

3.2. Thermogravimetric Analysis (TGA). TGA was conducted to evaluate the moisture content and the degradation stages of the drug, polymer, and loaded and unloaded discs. It is also used to determine the decomposition characteristics of the sample during heating. Thermograms of the HA, 5-ASA, loaded, and unloaded hydrogel discs from 0 to 500 °C are shown in Figure 2. The chemical composition and particle size are two typical characteristics that influence a substance's moisture content. Compared to a cross-linked polymeric system, HA showed broader particle size distributions. Furthermore, the structure of native HA is more hydrophilic as compared to the polymeric system due to the abundance of hydrophilic functional groups it contains, including −OH, −COO, and −NH groups.[19] Three stages were identified by the thermal analysis that is an initial mass loss associated with dehydration, a second stage associated with partial molecular structure breaking, and a third stage associated with hyaluronan residue degradation. The TGA

https://doi.org/10.1021/acsomega.4c03240
ACS Omega 2024, 9, 28827−28840

thermogram of HA revealed that weight loss between 44 and 145 °C was ascribed to water evaporation, while the partial molecular structural breakdown was observed between 290 and 434 °C. The essential structural framework of HA broke down between 488 and 498 °C, which resulted in C−O−C bond dissociation and subsequent weight loss.[39]

The thermogram of 5-ASA revealed a clear endothermic peak between the melting points of 355 and 285 °C. The physical mixes of 5-ASA and HA contained this acute endothermic peak, which had a temperature range of 266−409 °C. Similarly, a hydrogel TGA thermogram showed a very slight weight loss of up to 5% at 252 °C, which was attributed to polymer water loss. The temperature was then increased to 495 °C, and 87% weight loss was recorded. Subsequently, the hydrogel structure started to degrade and continued to do so until it was completely destroyed. The TGA thermograms of the individual reactants and the synthesized hydrogel thus indicated greater thermal stability in the polymeric hydrogels, suggesting that cross-linking and grafting enhanced the thermal stability of pure HA and the drug. Cross-linking, grafting, and polymerization resulted in enhanced thermal stability of the hydrogel, which exhibited significant intermolecular interactions with its constituents.[33] Our conclusions are supported by the findings of Bucak and co-workers, who developed hydrogel beads based on alginate and found that the substance improved the temperature stability of the hydrogel beads.[40]

3.3. Scanning Electron Microscopy (SEM). An immersion lens SEM detector was used to collect high-resolution surface imaging during the acquisition of micrographs of surface of hydrogels at various magnifications with an accelerating voltage of 15 kV. The micrographs in Figure 3

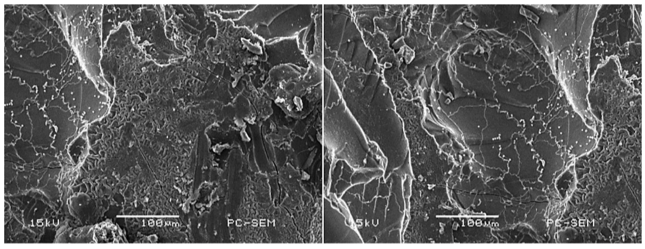

Figure 3. SEM images of the drug-loaded hydrogel disc.

show the porosity and more compact structure of the hydrogel, suggesting considerable interactions between the polymer and the combination of monomers as well as effective graft and cross-link copolymerization. These results provide an explanation for the slower disintegration rate of HA-AAc-MA hydrogels and the significant physical interaction between the polymer and the monomer.[33] The rough surface suggested that 5-amino salicylic acid adhered to the three-dimensional polymer network. Furthermore, the folds and cracks of the product would be the places where water could sweep in and interact with hydrophilic groups in the three-dimensional polymer network.[37]

3.4. Powder X-ray Diffraction (PXRD) Analysis. Improved aqueous solubility and significant bioavailability are the main benefits of the amorphous form of the delivery system.[28] The crystallinity or amorphous nature of the drug, polymer, and drug-loaded polymeric network were examined using PXRD. When a substance is amorphous rather than crystalline, its solubility is greater. Amorphous structures are required to improve water solubility in drug delivery systems intended to deliver BCS class IV drugs.[41] Figure 4 depicts the PXRD of polymer (a), drug (b), and drug-loaded hydrogel (c). PXRD analysis of 5-amino salicylic acid revealed prominent, significant peak values at 14.52, 15.96, 26.52, and 27.68°, indicating that the drug has a highly crystalline configuration, as shown in Figure 4. PXRD analysis of HA revealed peaks at 2θ = 10.08, 13.24, 18.32, 24.76, 32.40, and 31.12°. However, in the PXRD analysis of the drug-loaded hydrogels, the characteristic peaks of the reactants and the drug were not observed. The prominent and powerful peaks of the loaded drug were attributed to the amorphous structure of the polymeric network. 5-Amino salicylic acid was successfully loaded into the hydrogels, as evidenced by a decrease in the peak intensity of the drug. Compared with crystalline substances, amorphous systems provide a superior platform for enhancing certain attributes, such as solubility and dissolution rate, because they have higher molecular mobility and intermolecular energy levels.[35] The drug molecules filled the hydrogel spaces, and the structural integrity of the drug was preserved. However, the crystallinity of the drug decreased due to fewer electrostatic attractions, which are caused by fewer inter- and intramolecular attraction forces.[42]

3.5. Sol−Gel Fraction. The "sol fraction" refers to the portion of the hydrogels that are not completely cross-linked, whereas the cross-linked fraction is referred to as the "gel fraction" due to interactions between the polymer, monomer, and cross-linker during the polymerization process. The partial segment of the hydrogel that remains uncross-linked after different components are integrated is known as the sol fraction. This is because there were no reactive sites present during the polymerization process.[43] Weighed hydrogel discs were extracted using the Soxhlet method, and discs with varying formulations were used to evaluate the impact of HA, MA, AAc, and MBA on the sol and gel fractions; the results are shown in Figure 5. As the HA concentration increased in the CM-1 to CM-3 formulations, the gel percentage increased from 70 to 76%. A greater amount of available carboxyl and hydroxyl groups on the polymers led to an increase in the number of reactive sites, which led to an increase in the gel fraction with increasing polymer concentrations. As the concentrations of AAc and MA increased, the gel fraction in formulations CM-4 to CM-6 increased from 73 to 85%. An increased number of carboxyl groups as reactive sites are linked to higher monomer concentrations. A greater contact between the polymer and the monomers results in an increase in the number of reactive sites, which increases the gel content. Similarly, formulations CM-7 and CM-9 exhibited gel percentages that increased from 73 to 78% with increasing MBA content. This was explained by the network's higher cross-linking density being driven by the gradual increase in the amount of MBA.[44] Noreen S. and associates designed pH-sensitive chemically cross-linked block copolymers and reached the same conclusions as our research.[39] In the overall study, the CM-6 formulation showed a significant difference in the gel fraction compared to that of the other formulations, which may be associated with the highest concentration of the monomers, which provided sufficient functional groups for the reaction.

3.6. Swelling Studies. Swelling leads to substantial drug release from the network, proving that it plays a crucial role in the release of the drug from the polymeric network. Investigations on swelling were carried out in simulated gastric conditions like colon, small intestine, duodenum, and stomach with buffers of different pH like 7.4, 6.8, 4.5, and 1.2,

https://doi.org/10.1021/acsomega.4c03240
ACS Omega 2024, 9, 28827−28840

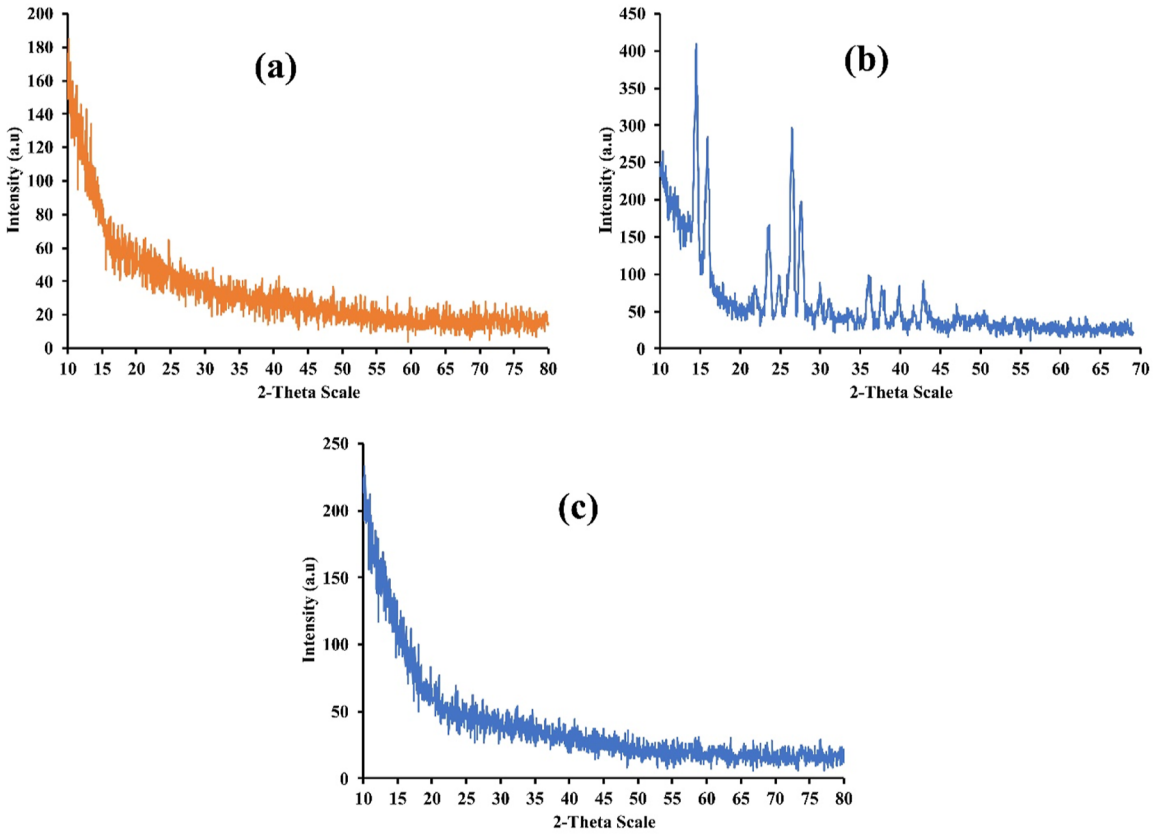

Figure 4. PXRD analysis of the polymer (a), drug (b), and drug-loaded hydrogels (c).

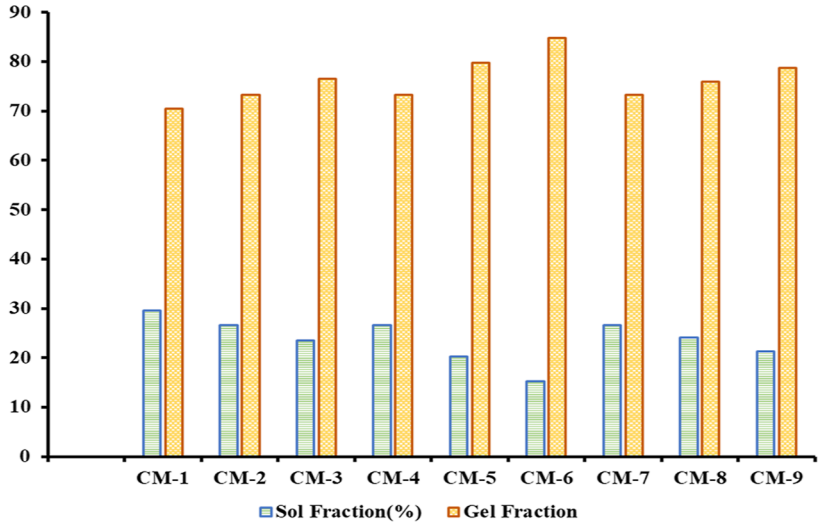

Figure 5. Sol−gel fraction of the optimized formulation after complete drying.

respectively, as shown in Figure 6. The impacts of varying ratios of polymers, monomers, and cross-linkers were examined in addition to the influence of pH on hydrogel swelling. Increasing the pH had a major effect on the tendency of the hydrogels to swell. One possible explanation for the greater propensity of the hydrogels to swell at pH 7.4 and 6.8 than at pH 1.2 and 4.5 is the deprotonation of the carboxyl groups within the hydrogel network, which results in their transformation into carboxylate anions (COO−). Electrostatic repulsion between carboxylate anions (COO−) causes the network to expand significantly. Osmotic pressure, on the other hand, has been shown to support the enhanced swelling properties of hydrogels. Significant swelling was observed in buffer media with a pH of 7.4 due to intraionic repulsion between unprotonated carboxyl groups. Moreover, in aqueous or basic environments, carboxylate anions (COO−) in the hydrogel polymeric network have a significantly better solvation capability than nonionic groups. This characteristic led to the detection of significant swelling at pH 7.4 compared to SGF at pH 1.2.[45] However, based on the data presented in Figure 6, the swelling difference between 1.2 and 4.5 was comparable. Similarly, same effect was observed in pH 6.8 and

https://doi.org/10.1021/acsomega.4c03240
ACS Omega 2024, 9, 28827−28840

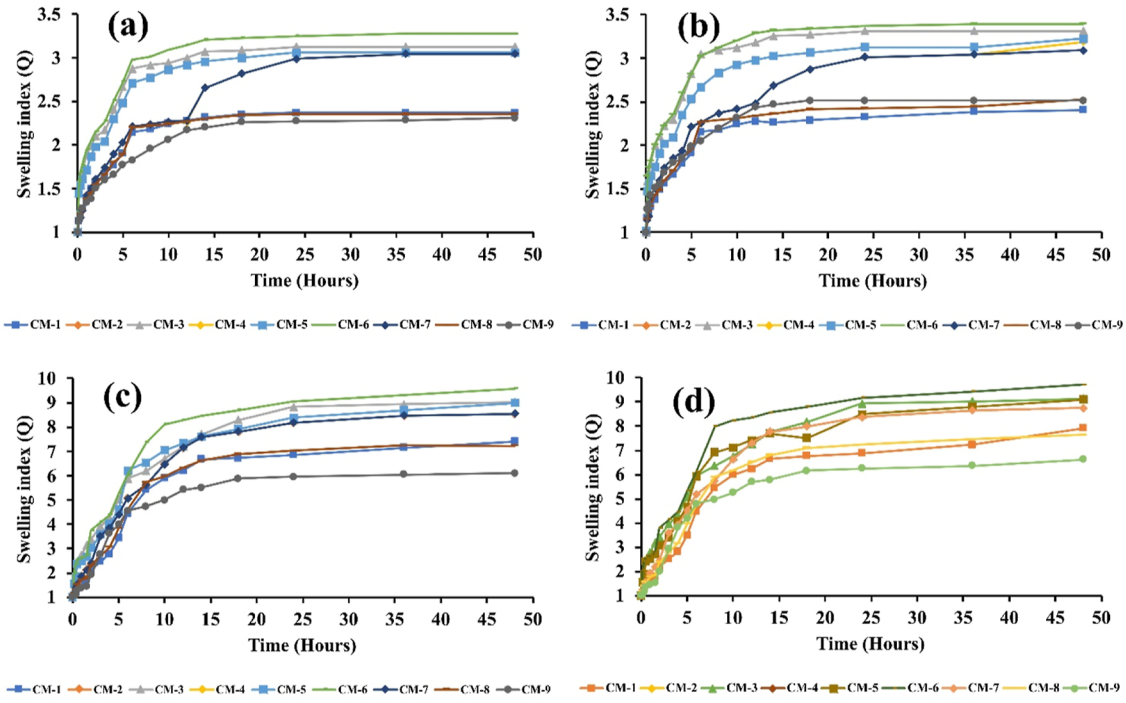

Figure 6. Swelling indices of hydrogels at pH 1.2 (a), pH 4.5 (b), pH 6.8 (c), and pH 7.4 (d).

7.4. The effects of varying concentrations of the constituents on hydrogel swelling were investigated while the hydrogels were formulated using various ratios of hyaluronic acid, methylenebis(acrylamide), methacrylic acid, and acrylic acid. When the polymer concentration increased from CM-1 to CM-3, the swelling tendency of the hydrogels increased. The presence of substantial amounts of hydrophilic moieties in the cross-linked network by increasing the polymer concentration led to excessive swelling. The system continued to exhibit enhanced swelling as the number of hydrophilic moieties increased along with the diffusion of the swelling media inside the polymeric network. Similarly, increasing the concentration of the polymer resulted in a large number of functional units for grafting acrylic and methacrylic acids. All these factors increased the potential for enhanced swelling as the polymer content increased. A previous study revealed that an increase in the β-CD concentration triggered the expansion of the polymeric system.[35] Variations in swelling were dependent on the AAc and MA concentrations because these contain more ionizable functional groups (carboxylic groups). The outcome was more noticeable at higher pH values because the functional groups ionize when the pH of the gel is higher than its pK_a, increasing the hydrophilicity of the polymeric system. Higher concentrations of AAc and MA led to greater ionic contact between the monomers and the polymer. A lower pH induces less apparent swelling because the hydrogel network offers fewer empty spaces for water molecules, and the connected carboxylic groups provide intra- and intermolecular H-bonding. The primary force behind network expansion, however, was the increase in electrostatic repulsion between the dissociated carboxylate ions (−COO−) caused by the dissociation of the carboxylic groups along the network chains at higher pH. The growth of the network increased the proportion of open space between network chains that were accessible to water molecules, which caused enhanced swelling.[46]

The swelling of the hydrogels decreased as the concentration of MBA (cross-linker) increased. By serving as a bridge during the development of a polymer network, MBA enables the addition of several cross-linked sites, which reduces the number of pores created between network chains. Compared to hydrogels with lower cross-linker concentrations, hydrogels with higher cross-linker concentrations have more packed structures with smaller pore sizes, which may explain why the swelling behavior of these hydrogels decreases with increasing cross-linker concentration.[47] Restricted relaxation of the network chains was the outcome of the subsequent decrease in pore size, which led to delayed diffusion of the swelling media into the polymeric hydrogels. Thus, the cross-linker concentration led to a decrease in the extent of the hydrogel swelling.[48]

3.7. Polymer Volume Fraction. Based on the findings of triplicate studies, it was observed that the concentration of MBA was directly linked to the polymer volume fraction but inversely linked to the concentrations of hyaluronic acid, methacrylic acid, and acrylic acid. The average values are presented in Table 2. The polymer volume fraction varies at

Table 2. Polymer Volume Fraction of Hydrogel Discs at pH 1.2, 4.5, 6.8, and 7.4

formulation code	V_{eq} (pH 1.2)	$V_2 = 1/V_{eq}$ (pH 1.2)	V_{eq} (pH 7.4)	$V_2 = 1/V_{eq}$ (pH 7.4)
CM-1	2.89	0.346020761	9.85	0.101522843
CM-2	2.96	0.337837838	10.01	0.0999001
CM-3	3.12	0.320512821	10.97	0.091157703
CM-4	2.96	0.337837838	10.01	0.0999001
CM-5	3.08	0.324675325	10.45	0.09569378
CM-6	3.18	0.314465409	10.75	0.093023256
CM-7	2.96	0.337837838	10.01	0.0999001
CM-8	2.65	0.377358491	9.76	0.102459016
CM-9	2.54	0.393700787	9.61	0.104058273

https://doi.org/10.1021/acsomega.4c03240
ACS Omega 2024, 9, 28827−28840

different pH values. In acidic media, a higher polymer volume fraction was observed as compared to basic media, where a lower polymer volume fraction was noted. This is because hydrogels showed less swelling at acidic pH as opposed to basic pH.[49] Our findings were primarily consistent with those of Badshah et al. (2021), who developed porous and extremely responsive cross-linked β-cyclodextrin-based nanomatrices to enhance drug absorption and dissolution.[35]

3.8. Percent Water Content. Hyaluronic acid is a hydrophilic polymer that contains 5−15% water and tends to retain water even after complete drying. Determining the actual water content in the hydrogels was critical for setting up experiments with correct ratios. The concentration of the hydrophilic polymer was correlated with an increase in the percentage of water in the hydrogel network, as indicated in Table 3. When the monomer concentration increased, the proportion of the total water content increased. With increasing monomer concentration, the polymer concentration and water content correlated as the polymer/cross-linker concentration remained constant. Consequently, the percentage of water content did not change noticeably. The increased cross-linker content in the formulation leads to highly cross-linked formulations with thick, hard surfaces since these hydrogels had a lower percent water content than the previous polymer and monomer ratios. The percent drug loading was calculated using the percent water content, which was the primary parameter determining the percent drug loading after the percent water content of all the sets. Our findings are comparable to those of Khaliq T and colleagues, who generated biomimetic hyaluronic acid/alginate hydrogel membranes for faster diabetic wound regeneration.[50]

Table 3. Percent Water Content and Drug Loading of the Hydrogel Disc

formulation code	percent water content	drug loading
CM-1	12.82	71.89
CM-2	13.29	72.21
CM-3	13.85	74.64
CM-4	13.29	72.21
CM-5	13.42	76.58
CM-6	13.96	81.34
CM-7	13.29	72.21
CM-8	12.02	67.28
CM-9	11.46	66.43

3.9. Percent Drug Loading. Percent drug loading in hydrogels was accomplished by using the postloading technique. As indicated by Table 3, the drug-loading results were suitable for every formulation, with the exception of CM-8 and CM-9. All of the hydrogels contained more than 65% drugs. The formulation that produced the best results was CM-6, with a drug-loading percentage of approximately 81.34%. Significant carboxylic acid (COO−) pendent moieties were linked to MA and AAc, which ionized at basic pH. The resultant repulsive interactions aid in hydrogel swelling at pH 7.4, leading to the increased drug loading.[44]

A possible correlation may exist between the higher concentration of cross-linker and the minimal loading of the CM-8 and CM-9 formulations. Dense networks with relatively high cross-linker concentrations were produced. Thus, a tightly interconnected network makes it difficult for a solvent to travel throughout it easily. Reduced swelling in the system was also beneficial for drug loading and release. There was a limited percentage of drug loading in CM-8 and CM-9 since all of these factors affected the drug's profound loading in the system.

3.10. In Vitro Drug Release. The buffer medias of different pH like 1.2, 4.5, 6.8, and 7.4 were used for the drug release studies, as shown in Figure 7. Although there was no

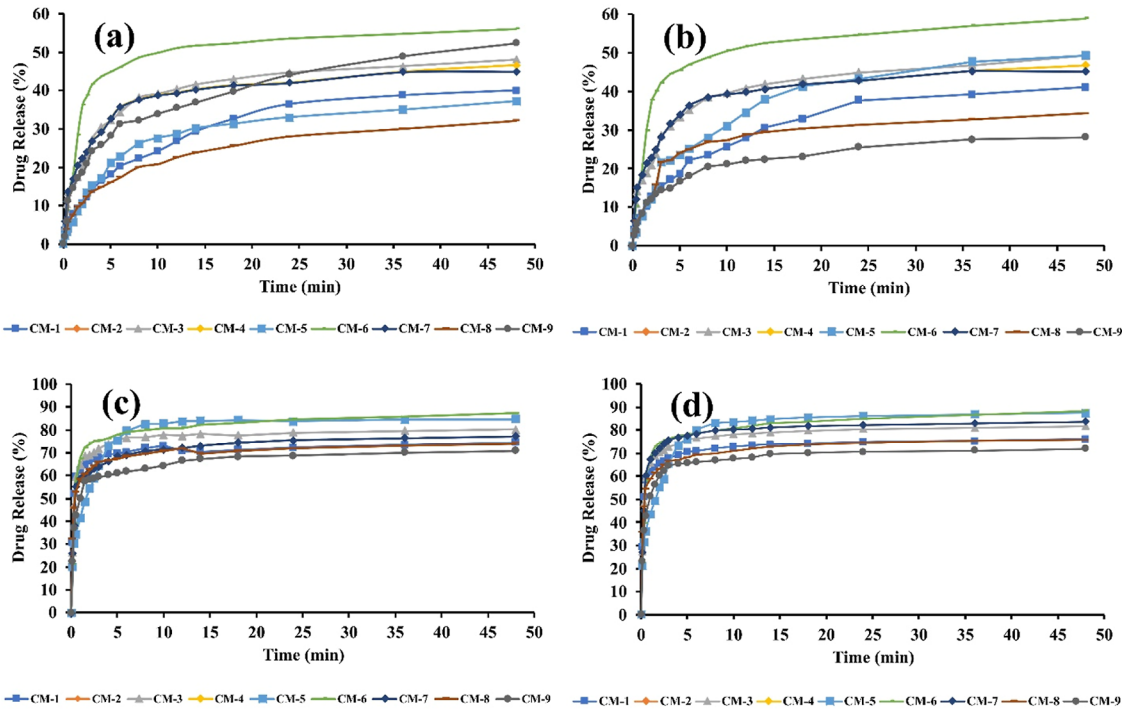

Figure 7. Drug release profiles of the formulated hydrogels at pH 1.2 (a), pH 4.5 (b), pH 6.8 (c), and 7.4 (d).

https://doi.org/10.1021/acsomega.4c03240
ACS Omega 2024, 9, 28827−28840

significant difference observed between drug release in pH 1.2 and 4.5 and in between 6.8 and 7.4 but based on the data presented in Figure 7, in comparison to 6.8 and 4.5, pH 7.4 produced the maximum drug release, while pH 1.2 produced the lowest drug release. Since network swelling at acidic pH was not significant, the compressed form of the drug prevented it from diffusing from the polymeric network more effectively. The basic media caused the polymeric network to swell and allowed water molecules to enter the cross-linked network. The drug molecules diffused significantly from the polymeric network in 20 min in pH 7.4 dissolution media (from hydrogels CM-1 to CM-7). Hydrogels likewise released 2−10% of the drug in 15 min in acidic media. Due to the excellent swelling ability and hydrophilic properties of the polymer, the polymer dissolved more quickly than did the drug. This activity affects the hydrodynamic layer around the hydrogels, which can lead to lower interfacial tension during dissolution. Similarly, by decreasing the 5-amino salicylic acid crystallinity and increasing the drug−hyaluronic acid interface, dissolution studies revealed that HA successfully enhanced the 5-ASA solubility profile. All of the formulations from 1 to 7 exhibited notable drug release. The amount of drug released from formulations 8 and 9 was reported to be limited as a result of the increased cross-linker concentration. This controlled release of the drug could be attributed to a highly organized and interconnected network. In contrast, the diffusion of dissolving media into the network was influenced by an increase in the cross-linker concentration, which formed a tight polymeric network with a relatively high cross-linking density and resulted in limited diffusion of the drug from the polymeric network. The in vitro drug release of the hydrogels was compared to that of Asacol, a commercially accessible 5-amino salicylic acid tablet. The highest release of the drug was observed in the two dissolving media, indicating that drug release from the hydrogels was efficient, whereas the release of the drug from commercially available tablets was delayed. The drug was continuously released from the commercial brand at pH 1.2 and 7.4, reaching its maximum release in an hour. At pH 1.2 and 7.4, the hydrogels showed fast and maximal drug release in 40 and 15 min, respectively.

3.11. Biocompatibility Studies. Toxicity studies were performed on healthy rabbits to assess the safety of the recently developed carrier system. Body weight, food and water consumption, fever, diarrhea, and ophthalmic and cutaneous toxicity were among the many parameters that were closely monitored during the course of the study. Table 4 shows that there were no appreciable differences in body weight or water or food consumption between the experimental and control groups. Hematological findings and various profiles of the liver, kidney, and lipids are shown in Tables 5 and 6. No alteration or variation was observed between the groups, confirming that the formulated system is safe and biocompatible with biological systems.

No animal group experienced any additional symptoms of illness. Tables 4 and 5 depict the results of hematological and biochemical analyses of blood samples from healthy individuals. Given that group B was provided hydrogels, which had increased white blood cell counts but remained within acceptable limits, the percentage of white blood cells in that group was relatively high. Moreover, kidney, liver, and lipid profiles of both the control and treated groups have been mentioned in Table 6 with no significant difference.

Table 4. Various Parameters of Both the Control and Tested Groups during the Biocompatibility Study

observations	group A (control)	group B (treated)
signs of illness	not observed	not observed
	Body Weight (kg)	
pretreatment	1.91 ± 0.04	1.98 ± 0.02
day 1	1.91 ± 0.02	1.99 ± 0.03
day 7	1.96 ± 0.03	2.03 ± 0.05
day 14	1.97 ± 0.02	2.11 ± 0.03
	Water Intake (ml)	
pretreatment	171.12 ± 1.18	182.11 ± 0.14
day 1	175.32 ± 1.16	186.23 ± 1.24
day 7	195.18 ± 3.16	197.41 ± 1.27
day 14	206.05 ± 3.21	210.21 ± 3.41
	Food Intake (g)	
pretreatment	74.32 ± 1.21	78.67 ± 1.05
day 1	75.11 ± 1.12	79.12 ± 1.04
day 7	76.25 ± 1.32	83.24 ± 1.33
day 14	79.21 ± 1.21	88.17 ± 1.55
dermal toxicity	not seen	not seen
ocular toxicity	absent	absent
mortality	nil	nil

The results represent the mean ± SD.

Table 5. Hematological Examination of Rabbit Blood

parameters	group A (control)	group B (treated)
hemoglobin (g/dL)	12.02	12.11
pH	7.15 ± 0.13	7.17 ± 0.11
white blood cells ($\times 10^9$ L^{-1})	5.1 ± 0.12	6.7 ± 0.15
red blood cells ($\times 10^6/\mu L$)	4.96 ± 1.11	5.01 ± 1.45
platelets ($\times 10^9$ L^{-1})	4.83 ± 0.13	4.88 ± 0.41
monocytes (%)	3.71 ± 0.25	3.79 ± 0.45
neutrophils (%)	51.45 ± 1.19	52.31 ± 2.15
lymphocytes (%)	45.25 ± 2.21	47.23 ± 2.76
mean corpuscular volume (%)	65.54 ± 2.23	66.11 ± 2.09
mean corpuscular hemoglobin (pg/cell)	24.71 ± 0.26	25.09 ± 3.08
mean corpuscular hemoglobin conc. (%)	33.22 ± 1.12	34.19 ± 1.71

The results represent the mean ± SD.

Table 6. Kidney, Liver, and Lipid Profiles of Both the Control and Treated Groups

biochemical analysis	group A (control)	group B (treated)
ALT (IU/L)	138.14 ± 1.66	148.15 ± 1.36
AST (IU/L)	39.11 ± 2.91	41.21 ± 2.61
urea (mmol/L)	16.12 ± 0.23	17.13 ± 1.21
creatinine (mg/dL)	1.19 ± 0.31	1.17 ± 0.38
uric acid (mg/dL)	4.07 ± 1.44	4.13 ± 1.81
cholesterol (mg/dL)	63.41 ± 2.41	65.12 ± 2.11
triglycerides (mg/dL)	62.12 ± 2.31	64.34 ± 3.36

The toxicity of the HA-AAc-MA gels has been assessed by histopathological examination of key organs. The animals were slaughtered on the 14th day of the experiment (Figure 8); the organs were removed and preserved in jars with a 10% formalin solution. As illustrated in Figure 9, H&E-stained tissue slides have been prepared in order to conduct histological examination of the aforementioned organs. Investigation findings revealed that the tissues of the essential

https://doi.org/10.1021/acsomega.4c03240
ACS Omega 2024, 9, 28827−28840

Figure 8. Animals slaughtered for organ extraction for histopathological studies (Photograph courtesy of Syed Faisal Badshah and Huma Liaqat, Copyright 2024).

organs (both the control and treated groups) exhibited no signs of deterioration, lesions, or other illnesses. The liver sections of both groups had inflammatory cell deposits and moderate hyperplasia. Heart tissues showed a characteristic pattern of cardiomyocytes without any signs of myocardial infarction or hypertrophy cells. A histological analysis of the lung tissues showed no lung fibrosis, but both groups had moderate edema and alveolar accumulation. Animal colons and intestines have been reported to be normal, showing no signs of inflammation. There was typical columnar epithelium, and the muscularis was intact. A microscopic examination of the kidneys showed that the tubules, Bowman capsule, and glomerulus were all in good condition. There was also a normal-looking spleen visible, with white blood cells evenly distributed throughout the white pulp. The groups treated with HA-AAc hydrogels and the control group did not differ significantly. In 2022, U. Rehman and colleagues designed hydrogels that are sensitive to pH with the objective of administering capecitabine while also conducting toxicity tests on rabbits. As we could see from our analysis, their findings were quite comparable.[51] A similar study was also performed by Badshah et al., and no toxic effect was observed.[52]

4. CONCLUSIONS

The successful synthesis of hydrogels from hyaluronic acid and combination monomers (acrylic acid and methacrylic acid) has accomplished which has opened up new possibilities for the treatment of IBD. The development of these hydrogels offers a promising approach for targeted drug delivery and controlled release within the gastrointestinal tract. Moreover, the use of hyaluronic acid provides biocompatibility and biodegradability, making hydrogels a safe option for medical applications.

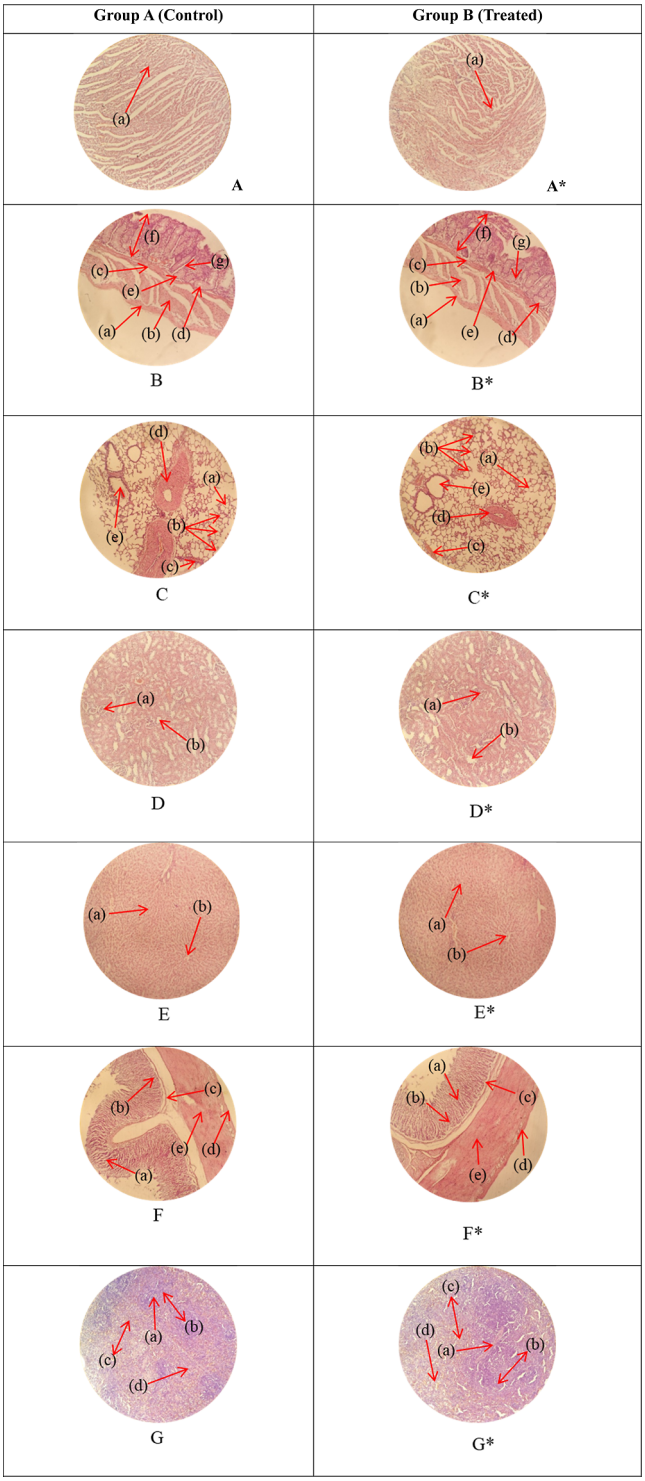

Figure 9. Histopathology of heart (A, A*): cardiac muscle fibers (a). Colon (B, B*): serosa (a), muscularis externa (b), muscularis mucosa (c), lumen of crypt (d), colonic crypt (e), mucosa (f), and lamina propria (g). Lungs (C, C*): alveolus (a), alveoli (b), blood vessel (c), pulmonary vessel (d), and bronchiole (e). Kidney (D, D*): glomerulus (a), and renal tubules (b). Liver (E, E*): plates of hepatocytes (a), and blood vessels (b). Small intestine (F, F*): small intestinal villi (a), intestinal gland (b), muscularis mucosa (c), serosa (d), and muscularis externa (e). Spleen (G, G*): central arteriole (a), white pulp (b), red pulp (c), and trabecular (d).

Furthermore, the combination of acrylic acid and methacrylic acid enables the customization of hydrogel properties, and this

https://doi.org/10.1021/acsomega.4c03240
ACS Omega 2024, 9, 28827−28840

versatility allows for tailored formulations that can adapt to the dynamic environment of the gastrointestinal tract, providing sustained and localized therapy. Compatibility of the constituents with one another and that of the drug with the hydrogels was confirmed by FTIR spectroscopy. A porous and rough morphology of the system was depicted by SEM. Moreover, an amorphous system was described by PXRD studies. The fabricated hydrogel was found to be pH-responsive, as evidenced by the swelling and drug release observed at pH 7.4 > 6.8 > 4.6 > 1.2. The hydrogels had the potential to swell to its full capacity at high pH, as observed in swelling, and a significant drug release was observed at higher pH as compared to lower pH. Similarly, the system was marked as biocompatible by toxicity studies as neither any sign of toxic effect on any organ nor any mortality was observed. In conclusion, the successful synthesis of these hydrogels holds great potential for advancing the field of IBD treatment, offering a platform for the development of innovative therapies with enhanced efficacy and reduced side effects. Further research and clinical studies are warranted to explore the full impact of these hydrogels in the context of IBD management.

AUTHOR INFORMATION

Corresponding Author

Syed Faisal Badshah − *Department of Pharmacy, Faculty of Medical and Health Sciences, University of Poonch, Rawalakot, Azad Jammu and Kashmir 12350, Pakistan;* orcid.org/0000-0001-7841-2038; Phone: +92-322-9827250; Email: faisal.badshah@upr.edu.pk

Authors

Huma Liaqat − *Faculty of Pharmacy, University of Lahore, Lahore 54590, Pakistan*

Muhammad Usman Minhas − *College of Pharmacy, University of Sargodha, Sargodha 40162, Pakistan;* orcid.org/0000-0001-7313-8500

Kashif Barkat − *Faculty of Pharmacy, University of Lahore, Lahore 54590, Pakistan; Faculty of Health Sciences, Equator University of Science and Technology, Masaka 961105, Uganda*

Saeed Ahmad Khan − *Department of Pharmacy, Kohat University of Science and Technology, Kohat 26000, Pakistan;* orcid.org/0000-0001-5606-2719

Muhammad Delwar Hussain − *Department of Pharmaceutical Sciences, School of Pharmacy and Health Professions, University of Maryland Eastern Shore, Princess Anne, Maryland 21853, United States*

Mohsin Kazi − *Department of Pharmaceutics, College of Pharmacy, King Saud University, Riyadh 11451, Saudi Arabia*

Complete contact information is available at: https://pubs.acs.org/10.1021/acsomega.4c03240

Notes

The authors declare no competing financial interest.

ACKNOWLEDGMENTS

The authors would like to extend their sincere appreciation to the Researchers Supporting Project Number (RSP2024R301), King Saud University, Riyadh, Saudi Arabia. All authors are thankful to the Faculty of Pharmacy, University of Lahore and Department of Pharmacy, University of Poonch, Rawalakot for providing financial and lab facilities.

REFERENCES

(1) Grossberg, L. B.; Papamichael, K.; Cheifetz, A. S. Review article: emerging drug therapies in inflammatory bowel disease. *Aliment. Pharmacol. Ther.* **2022**, *55* (7), 789−804.

(2) Le Berre, C.; Roda, G.; Nedeljkovic Protic, M.; Danese, S.; Peyrin-Biroulet, L. Modern use of 5-aminosalicylic acid compounds for ulcerative colitis. *Expet Opin. Biol. Ther.* **2020**, *20* (4), 363−378.

(3) Shahdadi Sardo, H.; Saremnejad, F.; Bagheri, S.; Akhgari, A.; Afrasiabi Garekani, H.; Sadeghi, F. A review on 5-aminosalicylic acid colon-targeted oral drug delivery systems. *Int. J. Pharm.* **2019**, *558*, 367−379.

(4) Cevallos, S. A.; Lee, J. Y.; Velazquez, E. M.; Foegeding, N. J.; Shelton, C. D.; Tiffany, C. R.; Parry, B. H.; Stull-Lane, A. R.; Olsan, E. E.; Savage, H. P.; et al. 5-Aminosalicylic acid ameliorates colitis and checks dysbiotic Escherichia coli expansion by activating PPAR-γ signaling in the intestinal epithelium. *Mbio* **2021**, *12* (1), No. e03227-20.

(5) Park, H.; Otte, A.; Park, K. Evolution of drug delivery systems: From 1950 to 2020 and beyond. *J. Controlled Release* **2022**, *342*, 53−65.

(6) Zeb, A.; Gul, M.; Nguyen, T. T. L.; Maeng, H. J. Controlled release and targeted drug delivery with poly (lactic-co-glycolic acid) nanoparticles: Reviewing two decades of research. *J. Pharm. Invest.* **2022**, *52* (6), 683−724.

(7) Sadozai, S. K.; Khan, S. A.; Karim, N.; Becker, D.; Steinbrück, N.; Gier, S.; Baseer, A.; Breinig, F.; Kickelbick, G.; Schneider, M. Ketoconazole-loaded PLGA nanoparticles and their synergism against Candida albicans when combined with silver nanoparticles. *J. Drug Delivery Sci. Technol.* **2020**, *56*, 101574.

(8) Laffleur, F.; Keckeis, V. Advances in drug delivery systems: Work in progress still needed? *Int. J. Pharm.* **2020**, *590*, 119912.

(9) Bordbar-Khiabani, A.; Gasik, M. Smart hydrogels for advanced drug delivery systems. *Int. J. Mol. Sci.* **2022**, *23* (7), 3665.

(10) Fitipaldi, H.; McCarthy, M. I.; Florez, J. C.; Franks, P. W. A global overview of precision medicine in type 2 diabetes. *Diabetes* **2018**, *67* (10), 1911−1922.

(11) Abbas, M. N.; Khan, S. A.; Sadozai, S. K.; Khalil, I. A.; Anter, A.; Fouly, M. E.; Osman, A. H.; Kazi, M. Nanoparticles Loaded Thermoresponsive In Situ Gel for Ocular Antibiotic Delivery against Bacterial Keratitis. *Polymers* **2022**, *14* (6), 1135.

(12) Caballero, D.; Abreu, C. M.; Lima, A. C.; Neves, N. M.; Reis, R. L.; Kundu, S. C. Precision biomaterials in cancer theranostics and modelling. *Biomaterials* **2022**, *280*, 121299.

(13) Lin, X.; Wang, X.; Zeng, L.; Wu, Z. L.; Guo, H.; Hourdet, D. Stimuli-responsive toughening of hydrogels. *Chem. Mater.* **2021**, *33* (19), 7633−7656.

(14) Pal, S.; Mehta, D.; Dasgupta, U.; Bajaj, A. Advances in engineering of low molecular weight hydrogels for chemotherapeutic applications. *Biomed. Mater.* **2021**, *16* (2), 024102.

(15) Fang, Z.; Chen, P.; Ji, Q.; Yan, C.; Gong, A. Stimuli-responsive hydrogel for disease therapy. *Polym. Bull.* **2023**, *81*, 1981−2000.

(16) Khan, S. A.; Schneider, M. Nanoprecipitation versus two step desolvation technique for the preparation of gelatin nanoparticles. In *Colloidal Nanocrystals for Biomedical Applications VIII*; SPIE, 2013.

(17) Barroso, N.; Guaresti, O.; Pérez-Álvarez, L.; Ruiz-Rubio, L.; Gabilondo, N.; Vilas-Vilela, J. L. Self-healable hyaluronic acid/chitosan polyelectrolyte complex hydrogels and multilayers. *Eur. Polym. J.* **2019**, *120*, 109268.

(18) Al-Bayaty, F.; Abdulla, M.; Darwish, P. Evaluation of hyaluronate anti-ulcer activity against gastric mucosal injury. *Afr. J. Pharm. Pharmacol.* **2009**, *5* (1), 23−30.

(19) Nikjoo, D.; van der Zwaan, I.; Brülls, M.; Tehler, U.; Frenning, G. Hyaluronic acid hydrogels for controlled pulmonary drug delivery—a particle engineering approach. *Pharmaceutics* **2021**, *13* (11), 1878.

(20) Cui, M.; Zhang, M.; Liu, K. Colon-targeted drug delivery of polysaccharide-based nanocarriers for synergistic treatment of inflammatory bowel disease: A review. *Carbohydr. Polym.* **2021**, *272*, 118530.

(21) Zhao, L.; Wang, F.; Cai, Z.; Zhou, Q.; Chen, B.; Zhang, C.; Liu, H.; Hong, L.; Zhang, T.; Zhong, J.; et al. Improving drug utilization platform with injectable mucoadhesive hydrogel for treating ulcerative colitis. *Chem. Eng. J.* **2021**, *424*, 130464.
(22) Vadlamudi, H. C.; Prasanna, R. Y.; Rubia, Y. B.; Vulava, J.; Vandana, K. In vitro characteristics of modified pulsincap formulation with mesalamine for ulcerative colitis treatment. *Indian Drugs* **2014**, *51* (03), 35−43.
(23) Sahar, F.; Riaz, A.; Malik, N. S.; Gohar, N.; Rasheed, A.; Tulain, U. R.; Erum, A.; Barkat, K.; Badshah, S. F.; Shah, S. I. Design, characterization and evaluation of gelatin/carboxymethyl cellulose hydrogels for effective delivery of ciprofloxacin. *Polym. Bull.* **2023**, *80* (11), 12271−12299.
(24) Erceg, T. D.; Vukić, N. R. Architecture of Hydrogels. In *Hydrogels*; CRC Press, 2023; pp 67−82.
(25) Rafique, N.; Ahmad, M.; Minhas, M. U.; Badshah, S. F.; Malik, N. S.; Khan, K. U. Designing gelatin-based swellable hydrogels system for controlled delivery of salbutamol sulphate: Characterization and toxicity evaluation. *Polym. Bull.* **2022**, *79* (7), 4535−4561.
(26) Moura, M. J.; Faneca, H.; Lima, M. P.; Gil, M. H.; Figueiredo, M. M. In situ forming chitosan hydrogels prepared via ionic/covalent co-cross-linking. *Biomacromolecules* **2011**, *12* (9), 3275−3284.
(27) Shah, S. A.; Sohail, M.; Minhas, M. U.; Nisar-ur-Rehman; Khan, S.; Hussain, Z.; Mudassir; Mahmood, A.; Kousar, M.; Mahmood, A. Retracted article: pH-responsive CAP-co-poly-(methacrylic acid)-based hydrogel as an efficient platform for controlled gastrointestinal delivery: fabrication, characterization, in vitro and in vivo toxicity evaluation. *Drug Delivery Transl. Res.* **2019**, *9*, 555−577.
(28) Chaala, M.; Sebba, F. Z.; Fuster, M. G.; Moulefera, I.; Montalbán, M. G.; Carissimi, G.; Víllora, G. Accelerated simple preparation of curcumin-loaded silk fibroin/hyaluronic acid hydrogels for biomedical applications. *Polymers* **2023**, *15* (3), 504.
(29) Zhang, M.; Chen, X.; Yang, K.; Dong, Q.; Yang, H.; Gu, S.; Xu, W.; Zhou, Y. Dual-crosslinked hyaluronic acid hydrogel with self-healing capacity and enhanced mechanical properties. *Carbohydr. Polym.* **2023**, *301*, 120372.
(30) Suhail, M.; Hsieh, Y. H.; Khan, A.; Minhas, M. U.; Wu, P. C. Preparation and In Vitro Evaluation of Aspartic/Alginic Acid Based Semi-Interpenetrating Network Hydrogels for Controlled Release of Ibuprofen. *Gels* **2021**, *7* (2), 68.
(31) Suhail, M.; Fang, C. W.; Chiu, I. H.; Hung, M. C.; Vu, Q. L.; Lin, I. L.; Wu, P. C. Designing and In Vitro Characterization of pH-Sensitive Aspartic Acid-Graft-Poly (Acrylic Acid) Hydrogels as Controlled Drug Carriers. *Gels* **2022**, *8* (8), 521.
(32) ASTM D *Standard test methods for laboratory determination of water (moisture) content of soil and rock by mass*; Astm West Conshohocken: PA, 2010.
(33) Suhail, M.; Shao, Y. F.; Vu, Q. L.; Wu, P. C. Designing of pH-Sensitive Hydrogels for Colon Targeted Drug Delivery; Characterization and In Vitro Evaluation. *Gels* **2022**, *8* (3), 155.
(34) Batool, N.; Sarfraz, R. M.; Mahmood, A.; Zaman, M.; Zafar, N.; Salawi, A.; Almoshari, Y.; Alshamrani, M. Orally Administered, Biodegradable and Biocompatible Hydroxypropyl−β−Cyclodextrin Grafted Poly (methacrylic acid) Hydrogel for pH Sensitive Sustained Anticancer Drug Delivery. *Gels* **2022**, *8* (3), 190.
(35) Badshah, S. F.; Akhtar, N.; Minhas, M. U.; Khan, K. U.; Khan, S.; Abdullah, O.; Naeem, A. Porous and highly responsive cross-linked β-cyclodextrin based nanomatrices for improvement in drug dissolution and absorption. *Life Sci.* **2021**, *267*, 118931.
(36) Pan, N. C.; Pereira, H. C. B.; da Silva, M. d. L. C.; Vasconcelos, A. F. D.; Celligoi, M. A. P. C. Improvement production of hyaluronic acid by Streptococcus zooepidemicus in sugarcane molasses. *Appl. Biochem. Biotechnol.* **2017**, *182*, 276−293.
(37) Laksanawati, T. A.; Trisanti, P. N.. Synthesis and characterization of composite gels starch-graftacrylic acid/bentonite (St-g-AA/B) using N'Nmethylenebisacrylamide (MBA). In *IOP Conference Series: Materials Science and Engineering*. IOP Publishing, 2019.
(38) Khan, R.; Zaman, M.; Salawi, A.; Khan, M. A.; Iqbal, M. O.; Riaz, R.; Ahmed, M. M.; Butt, M. H.; Alvi, M. N.; Almoshari, Y.; et al. Synthesis of chemically cross-linked pH-sensitive hydrogels for the sustained delivery of ezetimibe. *Gels* **2022**, *8* (5), 281.
(39) Noreen, S.; Pervaiz, F.; Ijaz, M.; Shoukat, H. Synthesis and characterization of pH-sensitive chemically crosslinked block copolymer [Hyaluronic acid/Poloxamer 407-co-poly (Methacrylic acid)] hydrogels for colon targeting. *Polym.-Plast. Technol. Mater.* **2022**, *61* (10), 1071−1087.
(40) Bucak, C. D. Porous alginate hydrogel beads cross-linked with citric acid containing tannic acid: structural analysis, antimicrobial properties and release behavior. *Cellulose* **2023**, *30* (2), 1117−1132.
(41) Boyd, B. J.; Bergström, C. A.; Vinarov, Z.; Kuentz, M.; Brouwers, J.; Augustijns, P.; Brandl, M.; Bernkop-Schnürch, A.; Shrestha, N.; Préat, V.; et al. Successful oral delivery of poorly water-soluble drugs both depends on the intraluminal behavior of drugs and of appropriate advanced drug delivery systems. *Eur. J. Pharm. Sci.* **2019**, *137*, 104967.
(42) Abbasi, M.; Sohail, M.; Minhas, M. U.; Khan, S.; Hussain, Z.; Mahmood, A.; Shah, S. A.; Kousar, M. Novel biodegradable pH-sensitive hydrogels: An efficient controlled release system to manage ulcerative colitis. *Int. J. Biol. Macromol.* **2019**, *136*, 83−96.
(43) Demeter, M.; Scărişoreanu, A.; Călina, I. State of the art of hydrogel wound dressings developed by ionizing radiation. *Gels* **2023**, *9* (1), 55.
(44) Aslam, A.; Ashraf, M. U.; Barkat, K.; Mahmood, A.; Hussain, M. A.; Farid-ul-Haq, M.; Lashkar, M. O.; Gad, H. A. Fabrication of Stimuli-Responsive Quince/Mucin Co-Poly (Methacrylate) Hydrogel Matrices for the Controlled Delivery of Acyclovir Sodium: Design, Characterization and Toxicity Evaluation. *Pharmaceutics* **2023**, *15* (2), 650.
(45) Bashir, S.; Hina, M.; Iqbal, J.; Rajpar, A. H.; Mujtaba, M. A.; Alghamdi, N. A.; Wageh, S.; Ramesh, K.; Ramesh, S. Fundamental concepts of hydrogels: Synthesis, properties, and their applications. *Polymers* **2020**, *12* (11), 2702.
(46) El-Sawy, N. M.; Raafat, A. I.; Badawy, N. A.; Mohamed, A. M. Radiation development of pH-responsive (xanthan-acrylic acid)/MgO nanocomposite hydrogels for controlled delivery of methotrexate anticancer drug. *Int. J. Biol. Macromol.* **2020**, *142*, 254−264.
(47) Haroon, B.; Sohail, M.; Minhas, M. U.; Mahmood, A.; Hussain, Z.; Ahmed Shah, S.; Khan, S.; Abbasi, M.; Kashif, M. U. R. Nano-residronate loaded κ-carrageenan-based injectable hydrogels for bone tissue regeneration. *Int. J. Biol. Macromol.* **2023**, *251*, 126380.
(48) Ali, A.; Haseeb, M. T.; Hussain, M. A.; Tulain, U. R.; Muhammad, G.; Azhar, I.; Hussain, S. Z.; Hussain, I.; Ahmad, N. A pH responsive and superporous biocomposite hydrogel of Salvia spinosa polysaccharide-co-methacrylic acid for intelligent drug delivery. *RSC Adv.* **2023**, *13* (8), 4932−4948.
(49) Saeed, S.; Barkat, K.; Ashraf, M. U.; Shabbir, M.; Anjum, I.; Badshah, S. F.; Aamir, M.; Malik, N. S.; Tariq, A.; Ullah, R. Flexible Topical Hydrogel Patch Loaded with Antimicrobial Drug for Accelerated Wound Healing. *Gels* **2023**, *9* (7), 567.
(50) Khaliq, T.; Sohail, M.; Minhas, M. U.; Mahmood, A.; Munir, A.; Qalawlus, A. H. M.; Jabeen, N.; Kousar, M.; Anwar, Z. Hyaluronic acid/alginate-based biomimetic hydrogel membranes for accelerated diabetic wound repair. *Int. J. Pharm.* **2023**, *643*, 123244.
(51) Rehman, U.; Sarfraz, R. M.; Mahmood, A.; Akbar, S.; E. Altyar, A.; Khinkar, R. M.; Gad, H. A. pH responsive hydrogels for the delivery of capecitabine: Development, optimization and pharmacokinetic studies. *Gels* **2022**, *8* (12), 775.
(52) Badshah, S. F.; Minhas, M. U.; Khan, K. U.; Barkat, K.; Abdullah, O.; Munir, A.; Suhail, M.; Malik, N. S.; Jan, N.; Chopra, H. Structural and *in-vitro* characterization of highly swellable β-cyclodextrin polymeric nanogels fabricated by free radical polymerization for solubility enhancement of rosuvastatin. *Part. Sci. Technol.* **2023**, *41*, 1131−1145.

https://doi.org/10.1021/acsomega.4c03240
ACS Omega 2024, 9, 28827−28840